Optics Letters

Measurement of the soliton number in guiding media through continuum generation

David Castelló-Lurbe,[1,*] **Antonio Carrascosa,**[2,3] **Enrique Silvestre,**[2,4]
Antonio Díez,[2,3] **Jürgen Van Erps,**[1] **Nathalie Vermeulen,**[1] **and**
Miguel V. Andrés[2,3]

[1]*Brussels Photonics (B-PHOT), Department of Applied Physics and Photonics, Vrije Universiteit Brussel, Pleinlaan 2, 1050 Brussel, Belgium*
[2]*Institut Universitari de Ciències dels Materials, Universitat de València, Catedrático Agustín Escardino 9, 46980 Paterna, Spain*
[3]*Departament de Física Aplicada i Electromagnetisme, Universitat de València, Dr. Moliner 50, 46100 Burjassot, Spain*
[4]*Departament d'Òptica, Universitat de València, Dr. Moliner 50, 46100 Burjassot, Spain*
Corresponding author: david.castello-lurbe@vub.be

No general approach is available yet to measure directly the ratio between chromatic dispersion and the nonlinear coefficient, and hence the soliton number for a given optical pulse, in an arbitrary guiding medium. Here we solve this problem using continuum generation. We experimentally demonstrate our method in polarization-maintaining and single-mode fibers with positive and negative chromatic dispersion. Our technique also offers new opportunities to determine the chromatic dispersion of guiding media over a broad spectral range while pumping at a fixed wavelength. © 2020 Optical Society of America

https://doi.org/10.1364/OL.399382

Nonlinear propagation of optical pulses in fibers or integrated waveguides allows widening pulse spectra, which can give rise to continuum generation (CG). These broadband light sources are employed in time-resolved spectroscopy owing to their pulsed nature [1]. In addition, some of the processes that take part in the CG also find other applications. During the first stage of pulse spectral broadening, pulses are frequency chirped and, consequently, can be shortened in either fiber [2] or external compressors [3]. In a second stage, new frequencies can be produced through dispersive wave emission (DWE), a mechanism that can be used for wavelength conversion [4]. Both nonlinear and dispersive effects generally play an important role in these phenomena [5]. Intuitively, one could expect that fiber or integrated waveguide properties involved in CG somehow imprint the output light. Certainly, if information about the guiding media could be extracted by comparing input and output pulses and their spectra, then CG would find another promising application in this domain. However, a fundamental limitation arises in the very beginning of this tentative approach. Usually, measurement methods are built on the basis of an analytical model that connects different experimentally accessible magnitudes. Unfortunately, the inherent complexity of CG, linked to the interplay between nonlinearities and dispersion, makes such a preliminary requirement quite challenging.

Existing techniques to determine the nonlinear coefficient γ in fibers make apparent this issue. These methods rely on measurements of the nonlinear phase, through either spectral analysis [6,7]—recently generalized to obtain both magnitude and sign of γ in integrated waveguides [8]—or interferometry [9], which disregards chromatic dispersion. This approximation can introduce a significant error in some cases, as studied in Ref. [10]. Contrary to low-power experiments, where dispersive processes dominate at any propagation distance, at high powers, the spectral broadening initially governed by nonlinear processes makes dispersive effects gradually more important. Although dispersion can be safely neglected with (quasi)continuous-wave (CW) pumping, the contributions of the Kerr effect and electrostriction cannot be separated under these conditions [11,12]. The Kerr nonlinearity can be isolated, while dispersive effects are avoided, based on measurements of polarization-state changes [13]. However, this approach requires cylindrical symmetry, which prevents its application in integrated waveguides.

Under specific conditions where the nonlinear Schrödinger equation (NLSE) can be analytically solved, measurements of γ can account for dispersion. For example, γ can be extracted from the spectral resonances produced during the initial stage of modulation instability [14,15] or by monitoring the power of idler frequencies obtained through four-wave mixing (FWM) pumped by tunable CW lasers [16]. In sharp contrast to these methods, where the use of analytical results is preferred over a wider application scope, a hybrid approach based on frequency resolved optical gating (FROG) and brute-force fittings to numerical solutions of the NLSE was also proposed to deal with nonlinear and dispersive effects simultaneously [17].

Here we propose, what is to our knowledge the first general approach to measure the coefficient β_2/γ, where β_2 is the group-velocity dispersion parameter, in an arbitrary guiding medium. Note that for a given input pulse, this coefficient provides the soliton number N straightforwardly, since $N^2 = T_0^2 \gamma P_0/|\beta_2|$, with T_0 and P_0 being the input pulse width

and peak power, respectively. As we will show, our method relies on a conservation law of the NLSE, so it is not limited to specific ranges of β_2 or γ values, unlike previous works [6–9,13–16]. In addition, contrary to Ref. [17], the experimental data can be fitted here to a fully analytical relation between readily accessible magnitudes, namely, the root-mean-square (rms) spectral width of the pulse and its intensity autocorrelation. We demonstrate our technique in polarization-maintaining (PM) fibers and (non-PM) single-mode fibers with well-known β_2/γ values, in both normal ($\beta_2 > 0$) and anomalous ($\beta_2 < 0$) dispersion regimes. Based on this wide applicability, we anticipate no major restrictions when applying our method in integrated waveguides where injection losses have been evaluated properly. Finally, new opportunities to determine higher-order coefficients, such as β_3/γ, where β_3 is the third-order dispersion (TOD) parameter, are envisaged through a generalization of the present work.

Let us assume a single-mode electric field propagating in a guiding medium in the z direction, $\mathbf{E}(x, y, z, t) = (1/2)A(z, T)\tilde{\mathbf{e}}(x, y, \omega_0)e^{-i\omega_0 t}e^{i\beta(\omega_0)z} + \text{c.c.}$, where $A(z, T)$ represents the complex envelope of the field, $\tilde{\mathbf{e}}(x, y, \omega_0)$ describes the electric-field mode, which is normalized such that $|A(z, T)|^2$ equals the instantaneous power, ω_0 denotes the mean frequency, β indicates the propagation constant, and $T = t - \beta_1 z$, with $\beta_m = d^m\beta/d\omega^m|_{\omega_0}$, is the time in the retarded frame. If $\beta(\omega) = \beta_0 + \beta_1(\omega - \omega_0) + (1/2)\beta_2(\omega - \omega_0)^2$, then $A(z, T)$ propagates according to the NLSE [5]:

$$\partial_z A = -\frac{\alpha}{2}A - i\frac{\beta_2}{2}\frac{\partial^2 A}{\partial T^2} + i\gamma|A|^2 A, \qquad (1)$$

where α is the loss coefficient. Starting from Ref. [18], we derive the following balance law for Eq. (1):

$$\frac{d}{dz}[\mathcal{L}_{NL}^{-1}(z) + \mathcal{L}_D^{-1}(z)] = -\alpha\mathcal{L}_{NL}^{-1}(z), \qquad (2)$$

where $\mathcal{L}_{NL}^{-1}(z) = (\gamma/2)\int_{-\infty}^{\infty}|A(z, T)|^4 dT / \int_{-\infty}^{\infty}|A(z, T)|^2 dT$; $\mathcal{L}_D^{-1}(z) = (\beta_2/2)\int_{-\infty}^{\infty}\Delta\omega^2|\tilde{A}(z, \Delta\omega)|^2 d\omega / \int_{-\infty}^{\infty}|\tilde{A}(z, \Delta\omega)|^2 d\omega$, with $\Delta\omega = \omega - \omega_0$ and $\tilde{A}$ being the Fourier transform of A. The z-dependent functions $\mathcal{L}_{NL}(z)$ and $\mathcal{L}_D(z)$ represent the length scales over which nonlinearities and dispersion act at *any* propagation distance and generalize the classical lengths $L_{NL} = 1/(\gamma P_0)$ and $L_D = T_0^2/|\beta_2|$ [18]. These functions have been very useful for solving several problems including DWE in both normal and anomalous dispersion regimes [19,20], shock waves [21,22], or dynamic control of the pulse chirp [8,23].

In this case, and for the sake of convenience, we integrate Eq. (2) over the guiding medium length L and write

$$-(\rho(L) - \rho(0)) - \alpha\int_0^L \rho(z)dz = \frac{\beta_2}{2\gamma}(\mu_2(L) - \mu_2(0)), \qquad (3)$$

where $\rho(z) = (1/2)\int_{-\infty}^{\infty}|A(z, T)|^4 dT / \int_{-\infty}^{\infty}|A(z, T)|^2 dT$ is proportional to the intensity autocorrelation at zero time delay, and $\mu_2(z) = \int_{-\infty}^{\infty}\Delta\omega^2|\tilde{A}(z, \Delta\omega)|^2 d\omega / \int_{-\infty}^{\infty}|\tilde{A}(z, \Delta\omega)|^2 d\omega$ is the square of the rms spectral width. In the context of nonlinear applications, typically $\alpha L \ll 1$, hence $\alpha\int_0^L \rho(z)dz \approx \alpha L(1/2)(\rho(L) + \rho(0))$. Consequently, if the path-independent quantities $\Delta\rho_{loss} = \rho(L) - \rho(0) +$
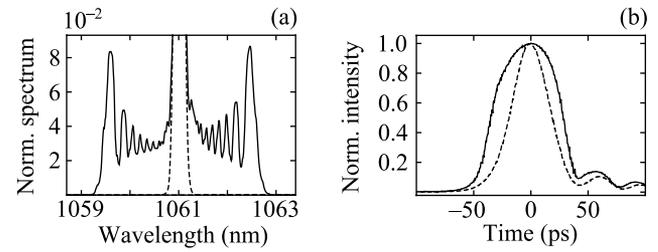

Fig. 1. (a) Spectrum and (b) pulse profiles at the input (dashed line) and output (solid line) of the 200 m long Nufern PM980-XP fiber pumped with 188 mW mean power. These results illustrate the spectrum and pulse evolutions for $\beta_2 > 0$.

$\alpha L(1/2)(\rho(L) + \rho(0))$ and $\Delta\mu_2 = \mu_2(L) - \mu_2(0)$ are defined, then Eq. (3) becomes

$$-\Delta\rho_{loss} = \frac{\beta_2}{2\gamma}\Delta\mu_2. \qquad (4)$$

Since an intensity autocorrelator, or even an oscilloscope in the case of relatively long pulses, provides ρ, and since μ_2 can be obtained by means of an optical spectrum analyzer (OSA), β_2/γ can be determined based on a linear fitting of $-\Delta\rho_{loss}$ as a function of $\Delta\mu_2$, according to Eq. (4). Importantly, as β_2 can be accurately measured at low powers using existing techniques [24], our approach to determine β_2/γ can also reduce the experimental uncertainty of γ in fibers or integrated waveguides.

Our first proof-of-concept experiment (PoCE) was carried out in a 200 m long PM optical fiber Nufern PM980-XP with α corresponding to $0.6\,\text{dB}\,\text{km}^{-1}$. A master-oscillator-fiber-amplifier laser built in the Laboratory of Fiber Optics at Universitat de València was used as the pump source. This laser emitted ~ 40 ps long pulses at 1061 nm and at a repetition rate of 23 MHz. Both laser and fiber output pulses were coupled into an OSA and a sampling oscilloscope to monitor their spectra and temporal power profiles (see Fig. 1) and evaluate $-\Delta\rho_{loss}$ and $\Delta\mu_2$.

In Fig. 2(a), $-\Delta\rho_{loss}$ is shown as a function of $\Delta\mu_2$ for a set of mean powers ranging from 51 mW to 379 mW. The linear relation between $-\Delta\rho_{loss}$ and $\Delta\mu_2$ predicted by Eq. (4) is observed, which allows measuring $\beta_2/\gamma = (6.3 \pm 0.1)\,\text{ps}^2$. To check the precision of our result, we compare the outcome of our experiment with a result calculated based on a measurement or nominal value of β_2 and γ (see Table 1). In this case, we also measured the chromatic dispersion of our PM980-XP fiber using an optical-fiber version of a standard interferometric technique [24], and obtained $\beta_2 = (24 \pm 2)\,\text{ps}^2\,\text{km}^{-1}$. Next, we calculate γ: hereto, we consider the mode field diameter MDF $= (6.6 \pm 0.5)\,\mu\text{m}$, as indicated in the fiber specifications (at 980 nm), and a reference value for the nonlinear index of standard fibers, $n_2 = 2.5 \times 10^{-20}\,\text{m}^2\,\text{W}^{-1}$ [5]. These values lead to $\gamma = (4.3 \pm 0.7)\,\text{W}^{-1}\,\text{km}^{-1}$, in line with the results obtained in Ref. [25] based on FWM experiments. Attending to these reference values, $\beta_2/\gamma = (5.6 \pm 1.4)\,\text{ps}^2\,\text{W}$, which agrees with our result. Therefore, our first PoCE in PM fiber gives very strong support to our approach.

In this experiment, the most important experimental source of error is related to power measurements (an accuracy of 5% in the power values is considered when fitting the experimental
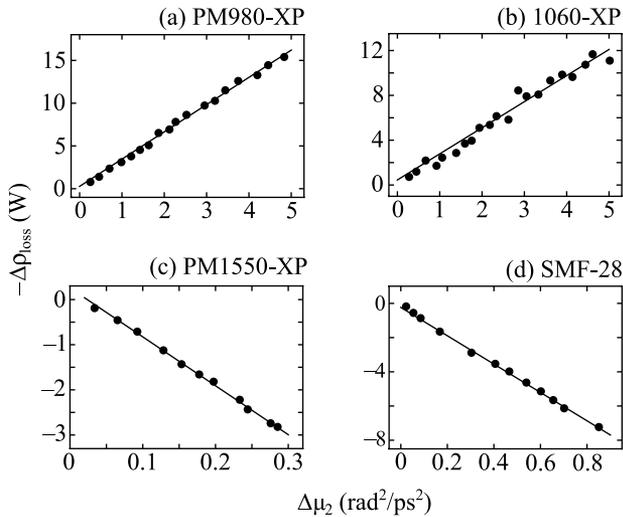
Fig. 2. Results of our experiments to determine β_2/γ in four different fibers: (a) PM fiber with $\beta_2 > 0$ at 1061 nm; (b) (non-PM) single-mode fiber with $\beta_2 > 0$ at 1061 nm; (c) PM fiber with $\beta_2 < 0$ at 1550 nm; and (d) (non-PM) single-mode fiber with $\beta_2 < 0$ at 1550 nm.

Table 1.   Comparison between Our Experimental Values for β_2/γ and Values Obtained Based on Fiber Specifications and Other Experiments (Details in the Text)

Fiber	Experimental β_2/γ (ps² W)	Nominal β_2/γ (ps² W)
PM980-XP	6.3 ± 0.1	5.6 ± 1.4
1060-XP	4.7 ± 0.2	4.5 ± 1.1
PM1550-XP	-21.7 ± 0.4	-21 ± 3
SMF-28	-16.6 ± 0.2	-18 ± 3

data). Nevertheless, the main intrinsic source of error in our approach is due to the approximation made to evaluate the loss contribution in $\Delta\rho_{\text{loss}}$. Attending to simulations based on Eq. (1), this error is smaller than 0.1% in this case. Accordingly, our approach can improve the accuracy of γ measurements, typically ~5% in short fibers where dispersion can be neglected and mean powers are measured with much higher accuracy [7], provided the uncertainty of power measurements and β_2 is less than 5%. If the loss contribution were larger, as may happen in integrated waveguides, then Eq. (4) would be used to obtain a first-order approximation of γ and subsequently evaluate $\int_0^L \rho(z)\mathrm{d}z$ numerically by means of Eq. (1). This process could then be iterated to improve the measurement of γ.

The second PoCE explored the viability of our method in a (non-PM) single-mode fiber. In single-mode fibers with randomly varying birefringence, the evolution of the electric field (averaged over the polarization states) is also governed by a NLSE-type equation where A and $|A|^2$ are replaced by $\mathbf{A} = (A_x, A_y)^T$ and $|A_x|^2 + |A_y|^2$, respectively, and γ is redefined as $(8/9)\gamma$ [5,26]. Therefore, Eq. (4) can also be derived for these fibers. Here we considered a 200 m long single-mode optical fiber Nufern 1060-XP with α corresponding to 0.9 dB km^{-1} (shorter or longer fiber lengths could also be considered).

This fiber was pumped with the same source employed in our first experiment at several mean powers between 57 mW and 352 mW. Spectra and pulse profiles were also measured analogously to the first case. The outcome of this second experiment is presented in Fig. 2(b), where $-\Delta\rho_{\text{loss}}$ also shows a linear dependence with respect to $\Delta\mu_2$. A linear fitting of these experimental points leads to $\beta_2/\gamma = (4.7 \pm 0.2)$ ps² W. To determine a reference value for β_2/γ, we considered $\beta_2 = (22 \pm 2)$ ps² km^{-1} based on the measurement carried out in Ref. [27] and we calculated $\gamma = (4.9 \pm 0.8)$ W^{-1} km^{-1} using the nominal value MFD $= (6.2 \pm 0.5)$ µm and the value of n_2 used for the PM980-XP fiber. These values result in $\beta_2/\gamma = (4.5 \pm 1.1)$ ps² W, also in accordance with our experimental value. In this way, we also demonstrated our approach in (non-PM) single-mode fibers.

So far, our experiments have been realized in the normal dispersion regime. Note that $\beta_2 > 0$ can be inferred from the positive sign of the line slopes observed in Figs. 2(a) and 2(b). To test our approach also in the anomalous dispersion regime, we repeated our measurement in a PM1550 fiber and a single-mode SMF-28 fiber pumped at 1550 nm. In this case, the experiments were realized in Brussels Photonics Laboratories at Vrije Universiteit Brussel using a Pritel PM femtosecond fiber laser emitting ~7 ps long pulses at a repetition rate of 60 MHz, and a FROG instrument (Coherent Solutions HR150) to characterize the pulse profiles. The results of our third PoCE with a 20 m long Nufern PM1550-XP fiber with α corresponding to 1 dB km^{-1} are plotted in Fig. 2(c). To produce appreciable pulse changes over the relatively short fiber length considered here, average powers ranging from 6 mW to 35 mW were employed. Furthermore, auxiliary fiber was required between the fiber under test (FUT) and the FROG device, which induced additional compression of the ps pulses and, as a result, an enlargement of $\rho(L)$. Consequently, the output pulses measured by means of the FROG setup were numerically propagated backwards along the auxiliary fiber to obtain $\rho(L)$ (leading to a reduction of about 32% in $\Delta\rho_{\text{loss}}$). On one hand, the experimental points in Fig. 2(c) fit very well to a line with a negative slope, which indicates $\beta_2 < 0$, as expected. On the other hand, the linear fitting provides $\beta_2/\gamma = (-21.7 \pm 0.4)$ ps² W. Attending to Ref. [28] and the specifications of the fiber, $\beta_2 = (26 \pm 2)$ ps² and MFD $= (10.1 \pm 0.4)$ µm, and thus, $\gamma = (1.3 \pm 0.1)$ W^{-1} km^{-1}, where the same n_2 value as in the previous experiments is considered. According to these reference values, $\beta_2/\gamma = (-21 \pm 3)$ ps² W, in line with the value obtained in our measurement. To complete our study in the anomalous dispersion regime, measurements in a 200 m long single-mode fiber Corning SMF-28 with α corresponding to 0.2 dB km^{-1} at mean powers from 1 mW to 3.4 mW were also performed. The evolution of the pulse spectrum and temporal profile corresponding to this experiment can be seen in Fig. 3. It is worth comparing the pulse compression observed in Fig. 3(b) for $\beta_2 < 0$, with the pulse broadening shown in Fig. 1(b) for $\beta_2 > 0$. The results of this fourth PoCE are plotted in Fig. 2(d) and yield $\beta_2/\gamma = (-16.6 \pm 0.2)$ ps² W (in this case, the reduction in $\Delta\rho_{\text{loss}}$ due to the auxiliary fiber being about 6% because significantly larger $\Delta\rho_{\text{loss}}$ values are achieved and the additional increase in $\rho(L)$ is much smaller compared to the third experiment). The fiber specifications indicate $\beta_2 = (21 \pm 2)$ ps² and MFD $= (10.4 \pm 0.5)$ µm, and thus,
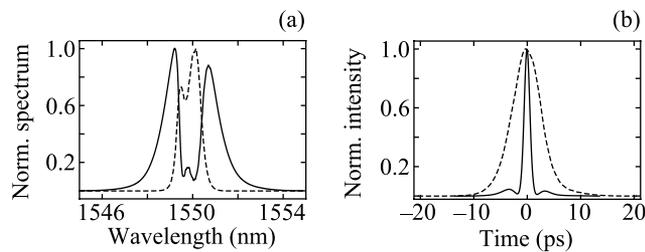
Fig. 3. (a) Spectrum and (b) pulse profiles at the input (dashed line) and output (solid line) obtained with 200 m long SMF-28 fiber pumped with 3.4 mW mean power. These results illustrate the spectrum and pulse evolutions for $\beta_2 < 0$.

$\gamma = (1.2 \pm 0.1)$ W^{-1} km^{-1} for the n_2 value used throughout this work. These values indeed correspond to those used to characterize a SMF-28 fiber in the modeling of the experiments in Ref. [29]. So, we can expect $\beta_2/\gamma = (-18 \pm 3)$ ps^2 W, which is also in excellent agreement with our result and thus proves our method in the anomalous dispersion regime. (An improved experimental arrangement enabling direct connection of the FUT to the measuring equipment would eliminate any requirement for numerical corrections, thus increasing even further the reliability of the technique.)

The measurements of β_2/γ reported here and the generalization of Eq. (2) and $\mathcal{L}_D^{-1}$ for guiding media where TOD becomes important enough (e.g., fibers pumped close to their zero dispersion wavelength) makes our approach promising to obtain β_3/γ based on pulse spectral asymmetries [18,20]. As such, one could obtain chromatic dispersion over the wavelength range spanned by the nonlinearly broadened spectrum, while pumping with a narrow-band pulse at a fixed wavelength. Further extensions to multimode guiding media might also be possible.

In conclusion, we have experimentally demonstrated that CG allows measuring β_2/γ in any single-mode fiber with a simple setup. Relying on an exact property of the equation that governs nonlinear pulse propagation, our method can also be applied in integrated waveguides. Moreover, in guiding media where chromatic dispersion has been precisely determined using other techniques, our method can rigorously remove fundamental error sources when measuring γ. Finally, our approach could give access to chromatic dispersion over a wide spectral range without the need to use tunable lasers or broadband sources that cover the wavelength range of measurement, and might also offer new ways for characterizing multimode guiding media.

REFERENCES

1. H. Tu and S. A. Boppart, Laser Photon. Rev. **7**, 628 (2013).
2. A. A. Amorim, M. V. Tognetti, P. Oliveira, J. L. Silva, L. M. Bernardo, F. X. Kärtner, and H. M. Crespo, Opt. Lett. **34**, 3851 (2009).
3. Y. Liu, H. Tu, and S. A. Boppart, Opt. Lett. **37**, 2172 (2012).
4. X. Liu, J. Læsgaard, U. Møller, H. Tu, S. A. Boppart, and D. Turchinovich, Opt. Lett. **37**, 2769 (2012).
5. G. P. Agrawal, *Nonlinear Fiber Optics*, 4th ed. (Academic, 2007).
6. Y. Namihira, A. Miyata, and N. Tanahashi, Electron. Lett. **30**, 1171 (1994).
7. A. Boskovic, S. V. Chernikov, J. R. Taylor, L. Gruner-Nielsen, and O. A. Levring, Opt. Lett. **21**, 1966 (1996).
8. N. Vermeulen, D. Castelló-Lurbe, J. L. Cheng, I. Pasternak, A. Krajewska, T. Ciuk, W. Strupinski, H. Thienpont, and J. Van Erps, Phys. Rev. Appl. **6**, 044006 (2016).
9. C. Vinegoni, M. Wegmuller, and N. Gisin, Electron. Lett. **36**, 886 (2000).
10. A. Lamminpää, T. Niemi, E. Ikonen, P. Marttila, and H. Ludvigsen, Opt. Fiber Technol. **11**, 278 (2005).
11. T. Kato, Y. Suetsugu, M. Takagi, E. Sasaoka, and M. Nishimura, Opt. Lett. **20**, 988 (1995).
12. D. Monzón-Hernández, A. N. Starodumov, Yu. O. Barmenkov, I. Torres-Gómez, and F. Mendoza-Santoyo, Opt. Lett. **23**, 1274 (1998).
13. J. Subías, J. Pelayo, R. Alonso, and F. Villuendas, J. Opt. Soc. Am. B **19**, 390 (2002).
14. M. Artiglia, E. Ciaramella, and B. Sordo, Electron. Lett. **31**, 1012 (1995).
15. J. Fatome, S. Pitois, and G. Millot, Opt. Fiber Technol. **12**, 243 (2006).
16. G. Huang, Y. Yamamoto, M. Hirano, A. Maruta, T. Sasaki, and K. Kitayama, Opt. Express **21**, 20463 (2013).
17. L. P. Barry, J. M. Dudley, P. G. Bolland, J. D. Harvey, and R. Leonhardt, Electron. Lett. **33**, 707 (1997).
18. D. Castelló-Lurbe, P. Andrés, and E. Silvestre, Opt. Express **21**, 28550 (2013).
19. D. Castelló-Lurbe and E. Silvestre, Opt. Express **23**, 25462 (2015).
20. D. Castelló-Lurbe, N. Vermeulen, and E. Silvestre, Opt. Express **24**, 26629 (2016).
21. A. Parriaux, M. Conforti, A. Bendahmane, J. Fatome, C. Finot, S. Trillo, N. Picqué, and G. Millot, Opt. Lett. **42**, 3044 (2017).
22. J. Nuño, C. Finot, G. Xu, G. Millot, M. Erkintalo, and J. Fatome, Commun. Phys. **2**, 138 (2019).
23. N. Vermeulen, D. Castelló-Lurbe, M. Khoder, I. Pasternak, A. Krajewska, T. Ciuk, W. Strupinski, J. Cheng, H. Thienpont, and J. Van Erps, Nat. Commun. **9**, 2675 (2018).
24. P. Hlubina, Opt. Commun. **193**, 1 (2001).
25. E. A. Zlobina, S. I. Kablukov, and S. A. Babin, Quantum Electron. **41**, 794 (2011).
26. D. Marcuse, C. R. Menyuk, and P. K. A. Wai, J. Lightwave Technol. **15**, 1735 (1997).
27. T. Zhang, Z. Yang, W. Zhao, Y. Wang, P. Fang, and C. Li, Chin. Opt. Lett. **8**, 262 (2010).
28. P. Morin, S. Boivinet, J.-P. Yehouessi, S. Vidal, T. Berberian, F. Druon, G. Machinet, F. Guichard, Y. Zaouter, and J. Boullet, Proc. SPIE **11357**, 1135715 (2020).
29. K. Hammani, B. Kibler, C. Finot, P. Morin, J. Fatome, J. M. Dudley, and G. Millot, Opt. Lett. **36**, 112 (2011).